Fibers and Polymers (2023) 24:921–929
https://doi.org/10.1007/s12221-023-00110-1

Online ISSN 1875-0052
Print ISSN 1229-9197

REGULAR ARTICLE

High Filterable Electrospun Nanofibrous Membrane with Charged Electret After Electrification Treatment for Air Filtration

Bo Yang[1] · Ming Hao[1,2] · Zheng Huang[1] · Zhijun Chen[1,2] · Yanbo Liu[1,2]

Received: 11 August 2022 / Revised: 11 October 2022 / Accepted: 12 October 2022 / Published online: 22 February 2023

Abstract

Conventionally, charged melt-blown nonwoven fabrics had been applied as filter media in various protective masks and high-temperature gas filters in relevant fields, which are featured with high filtration efficiency (FE) and low pressure drop (ΔP). The charges, however, and hence the filtration efficiency tend to decay with extended time, elevated temperature and increased humidity. In the current study, three types of charged nanofibrous membrane-based filtration medias, i.e., charged polyvinylidene fluoride (PVDF), polytetrafluoroethylene-PVDF, and tourmaline-PVDF electrospun nanofibrous membranes (ENMs), were successfully prepared by electrospinning process, followed by electrification. The resultant samples showed excellent filtration performance, relatively durable charging effect, and stable air permeability. Moreover, the data of FE and ΔP of ENMs after exposure to the air for 12 h are still more than 98% and less than 100 Pa, respectively. The combined method of electrospinning technology and electrification was proposed to obtain novel filter medias having semi-durable FE and relatively low ΔP, i.e., the FE will still remain at a relatively high level even if all the charges escape away from the nanofiber-based filter media, which may find wide applications in gas filtration industry.

Keywords Electrospun nanofibrous membrane · Electrification treatment · Filtration performance · Polyvinylidene fluoride · Polytetrafluoroethylene

1 Introduction

The term PM 2.5 is generally defined as the particulate matter with diameter equal to or less than 2.5 μm [1–3], which is mainly originated from industrial waste gas emissions, daily power generation, automobile exhaust, in the specific forms such as dust, sulfide, nitride, and organic hydrocarbon that diffuse into the air. It may raise the risk of diseases such as asthma, chronic bronchitis, and emphysema, even at a lower level of PM 2.5 [4, 5]. At present, a large number of base materials for industrial air filtration media are mainly glass fiber [6–8], as well as other high-performance-fiber nonwoven fabrics such as Kevlar, Nomex, due to its high-temperature resistance, dimensional stability, and high mechanical strength. But glass fiber is the extremely brittle inorganic material, which would break easily once bent. This can limit the application of glass fiber in flexible air filtration [9–11].

Another type of air filter is the fibrous filter, including melt-blown (MB) fibers and spunbonded fibers, which are attractive for particle filtration [12]. However, as for the size of particles are smaller than 500 nm, these filtration media cannot trap the particles in the air. In recent years, nanofibers have been used as part of filter media due to their high specific surface area and hence high filtration performance. Electrospinning technology is a special fibrous manufacturing process in which the droplet at the needle changes from a spherical shape to a conical shape and extends from the tip of the cone to obtain micro-nanofiber filaments under the strong electric field [13, 14]. Electrospun nanofibrous membranes (ENMs) have been investigated extensively for their potential applications in fields such as air filtration [15], battery separators [16], energy storage materials [17], biosensors

✉ Yanbo Liu
yanboliu@gmail.com

1 State Key Laboratory of New Textile Materials and Advanced Processing Technologies, School of Textile Science and Engineering, Wuhan Textile University, 1 Yangguang Avenue, Wuhan 430200, China

2 School of Textile Science and Engineering, Tiangong University, 399 Western Binshui Avenue, Tianjin 300387, China

[18], tissue engineering scaffolds [19], due to their advantages of micro-nano fiber diameter, high specific surface area, supreme porosity and interconnected pores [20–22]. Moreover, it can reduce the basis weight of ENM and effectively decrease the filtration resistance, while ensuring the full equivalent filtration efficiency.

Electrification treatment is a typical and efficient method for charging fibers with electret under the strong electrostatic force, resulting in good property of air filtration [23–25]. The electret fibers with high electric potential on its surface after electrification treatment can be used widely, due to the improved filtration efficiency as air filtration media [26–28]. It is reported that the particles in the air will be easily adsorbed and captured by the electrified fibers owing to the strong electrostatic force of permanent charges when passing through the electret filter medias [29–31]. Although initially the charged MB nonwoven filter media can achieve high efficiency and low resistance when used to filter the pollutant particulates in the air, the charges of these melt-blown fibers cannot be kept durably and easily escape to the air, due to the coarse fibers and the large pores in the melt-blown fabrics, elevated atmospheric temperature, humidity, air velocity, etc., resulting in a significant decrease in filtration efficiency [32].

Polyvinylidene fluoride (PVDF) has been widely used as air filtration media, owing to its low price, high toughness, good impact strength and excellent hydrophobic performance, which is very suitable for preparation of ENM by electrospinning technology. PVDF, Polytetrafluoroethylene (PTFE) and tourmaline are common and typical electret, due to their high charge storage capacity [33]. To obtain a high FE and semi-durable air filtration media, ENM with electrification treatment was deliberately designed in the current study. Herein, three types of ENMs, i.e., PVDF, PTFE-PVDF, and tourmaline-polyvinylidene difluoride (T-PVDF), were successfully prepared by combination of electrospinning technology and electrification treatment. The morphology, diameter, pore size, surface potential, filter performance and air permeability were subsequently studied. The resulting ENMs are expected to have high and semi-durable FE, low pressure drop (ΔP), compared to conventional MB nonwoven filter media. The semi-durable filtration effect is based on the small pore size of ENM which may still capture the PM 2.5 particles at high FE and low ΔP even if the charges on the resulting filtration media are partially or totally gone. The charges on MB web tend to decay with extended time, elevated temperature and increased humidity, the surface charges with strong electrostatic force cannot adsorb and capture particles in the air when passing through the nonwoven filter media.

2 Experimental

2.1 Materials

PVDF (molecular weight of 1,000,000) was purchased from Suzhou Qin Shang Plastic Chemical Co., Ltd. PTFE (molecular weight of 100,000, 100 nm) was supplied by DuPont, USA. Tourmaline (10,000 mesh) was provided by Shanghai Yaoyue New Material Technology Co., Ltd. polypropylene (PP) nonwoven fabric was supplied by Wuhan Winner Medical Co., Ltd. *N*, *N*-dimethylformamide (DMF), and acetone were purchased from Shanghai Maclean Biochemical Technology Co., Ltd. All chemicals were used without further purification.

2.2 Preparation of Spinning Solution

PVDF (12 wt%), *N*, *N*-Dimethylformamide (DMF, 30 mL), and acetone (10 mL) were added into a clean 100 mL flask with magnetic stirring at 50℃. After mixing for 30 min, PTFE (0.4 wt%) and tourmaline (0.4 wt% were slowly added into the mixed solution, respectively. The solution was kept for 4 h at 50 ℃ under agitation. After ultrasonic dispersion for 30 min, the PTFE-PVDF and tourmaline-PVDF (T-PVDF) spinning solution were obtained.

2.3 Preparation of ENM with Electrification Treatment

The preparation scheme of ENM with electrification treatment is shown in Fig. 1. The resulting ENMs were collected 20 cm apart from the needle tip on grounded metallic plate with a spunbonded PP nonwoven substrate (13 g/m^2) under 30/32 kV voltage and a feed rate of 1 mL/h. The electrospun membrane was electrified for 7 min, under − 8 kV charging voltage and 16 cm charging distance after collection. The ambient temperature was 25 ± 3 ℃ and the relative humidity was 30 ± 3%, when the ENMs were prepared.

2.4 Characterization

The surface morphologies of the ENMs were observed on a Nippon Electronics JSM6510 scanning electron microscope (SEM) which is a field emission scanning electron microscope (FESEM). The diameters of ENMs were measured by the software of Image Pro Plus on the recorded SEM photos. At least 50 nanofibers from each sample were randomly selected and analyzed. The pore sizes of the ENMs were recorded with a Gas–Liquid Pore Diameter Analyzer (model: CFP-1500A PMI), under the

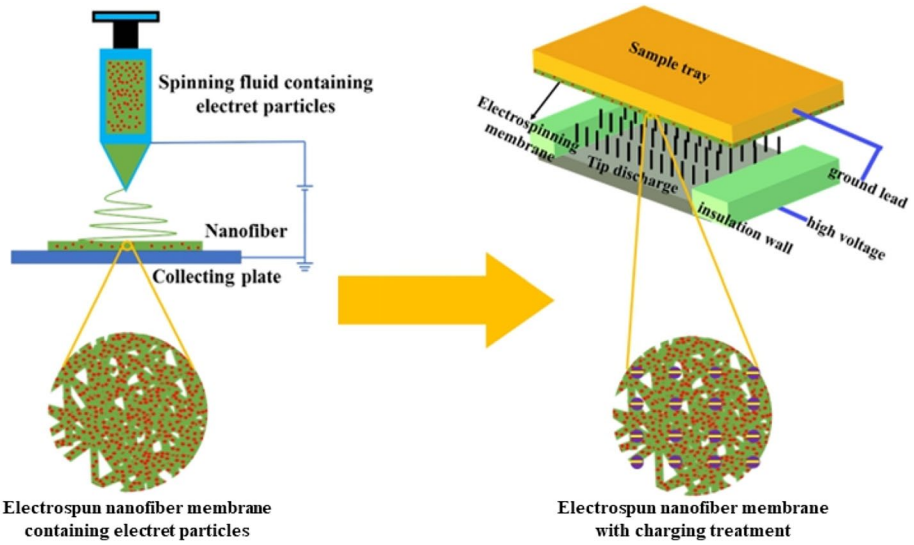

Fig. 1 Preparation scheme of ENM with electrification treatment

pressure of 0–60 psi. The surface potential of the ENM after electrification treatment was tested using the Electrostatic Tester (model: FMX-004). The filter performance was recorded on an Automatic Filter Material Tester (model: TSI8130), using salt aerosol (size: 0.26 μm) as the test carrier at the flow rate of 85 L/min with an effective area of 100 cm^2, according to the standard GBT13554-2008. Owing to the low strength of that, the ENM would be easily blown at the flow rate of 85 L/min. Therefore, two pieces of spunbonded PP nonwoven substrate with very low weight were used to cover both sides of the ENM before the test of the filtration performance [34, 35]. To evaluate the overall filtration performance of ENM, the filtration quality factor (QF) could be calculated by Eq. 1.

$$\mathrm{QF} = \frac{-\mathrm{In}(1-\mathrm{FE})}{\Delta P} \tag{1}$$

where FE and ΔP were the filtration efficiency and pressure drop of ENM, respectively. According to the standard ASTM D737-1996, the air permeability of the ENM was measured by Automatic Air Permeability Meter (model: YG461E-III) from Ningbo Textile Instrument Factory, China. Each reported value was the average of five valid specimens.

3 Results and Discussion

3.1 Morphology of ENM

Morphologies of ENM before and after electrification treatment were examined with FESEM (Fig. 2). It was noticeable that the surface morphology of PVDF ENMs did not change significantly after electrifying treatment in Fig. 2a, b. Similarly, Fig. 2c–f also show that corona charging has no significant effect on the apparent morphology of PTFE-PVDF and T-PVDF ENMs. The distribution of fiber diameters of ENMs before and after electrification treatment are shown in Fig. 3a–c, and the corresponding data are summarized in Table 1. As shown in Fig. 3a–c, average diameters of PVDF, PTFE-PVDF and T-PVDF ENMs before electrification treatment were 728 nm, 1125 nm and 555 nm, respectively, while average diameters of PVDF, PTFE-PVDF and T-PVDF ENMs after electrification treatment were 629 nm, 1086 nm, and 494 nm respectively. It was noteworthy that average diameters of the ENMs were almost smaller after electrification treatment. In fact, a large number of charged particles were attached to the traps on the surface of the ENM and the covalent bonds of the macro-molecules in the ENM, which were generated in the process of electrospinning. At the same time, charged particles in the ENM could be highly oriented in the electric field. When the sample was subjected to electret treatment, a large number of charges released by break of corona discharge, which would be continuously collected by samples. At the same time, the electric field would make the samples highly oriented with disordered and disordered dipoles. Therefore, under the function of electric field force, the nanofibers would be further drawn and thinned, resulting in the smaller fiber diameters.

The distribution of pore size of ENMs before and after electrification treatment were shown in Fig. 3d1–d3, and the corresponding data were summarized in Table 1. As shown in Fig. 3d1–d3, pore sizes of PVDF, PTFE-PVDF and T-PVDF ENM before electrification treatment were 1592 nm, 1793 nm and 1475 nm. While pore sizes of PVDF, PTFE-PVDF and T-PVDF ENM after electrification treatment were 1511 nm, 1766 nm and 1410 nm. As expected, pore sizes of ENMs almost became smaller after electrification treatment, like as the average fiber diameters.

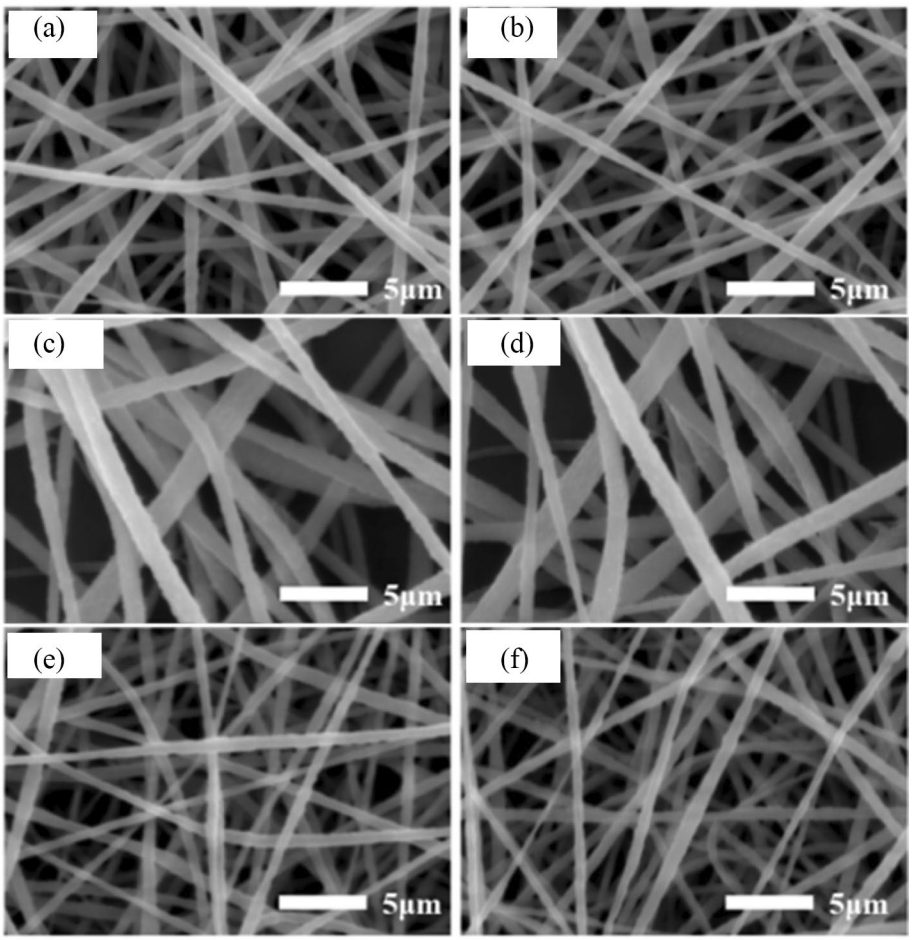

Fig. 2 FESEM photos of ENMs. **a** PVDF ENM; **b** polarized PVDF ENM; **c** PTFE-PVDF ENM; **d** polarized PTFE-PVDF ENM; **e** T-PVDF ENM; **f** polarized T-PVDF ENM

3.2 Surface Potential of ENM

Surface potential plays an important role for improving the filtration efficiency of ENM, owing to its permanent charges with strong electrostatic force to adsorb and capture particles in the air when passing through the electret filter media. Surface potential of three ENMs versus different charge voltages, with charging distance of 16 cm for 7 min at 25 ℃ and air relative humidity 30%, are shown in Fig. 4a–c. As shown from Fig. 4a, it was apparent that with the increase of charging voltage, the surface potential of three ENMs increased accordingly. When the charging voltage reached − 8 kV, the surface potential of ENMs tended to be stable. Herein, the surface voltage of PVDF, PTFE-PVDF, T-PVDF ENMs were about − 5 kV, − 3 kV, and − 6 kV. There are many small holes full of charge particles on the surface and interior of the ENM, and oriented electric dipoles inside the polymer at high voltages, resulting in creating the surface potential. Therefore, the higher the charging voltage, the stronger the electric field and the higher the potential on the surface. When the charging voltage is increased to a certain value, there is not any charge to be captured by ENM full of charge.

Surface potential of three ENMs against different charging distances, with charging voltage of − 8 kV for 7 min at 25 ℃ and air relative humidity 30%, are shown in Fig. 4b. As can be seen from Fig. 4b, when the distance was less than 18 cm, the surface potential of the three ENMs remained unchanged. When the charge distance was 20 cm, the surface potential of PVDF, PTFE-PVDF and T-PVDF ENM were − 3.2 kV, − 2.6 kV, and − 5.2 kV, which decreased by about 40.9%, 17.4%, and 16.8%, respectively. When the charging distance is short, the electric field is so strong that the corona charge device can generate enough charges to be captured by ENMs. However, when the charging distance continues to increase, the electric field strength will weaken, resulting in ENMs without enough charge.

Surface potential of three ENMs versus different charging time, with charging voltage of − 8 kV, charging distance of 16 cm at 25 ℃ and air relative humidity 30%, are shown in Fig. 4c. It was apparent that with the increase of charging time, the surface potential of three ENMs increased accordingly. However, the surface potential of ENMs tended to be stable and no longer increased with charge time, when the charging time increased to 7 min. Herein, the surface potential of PVDF, PTFE-PVDF, and T-PVDF ENMs were

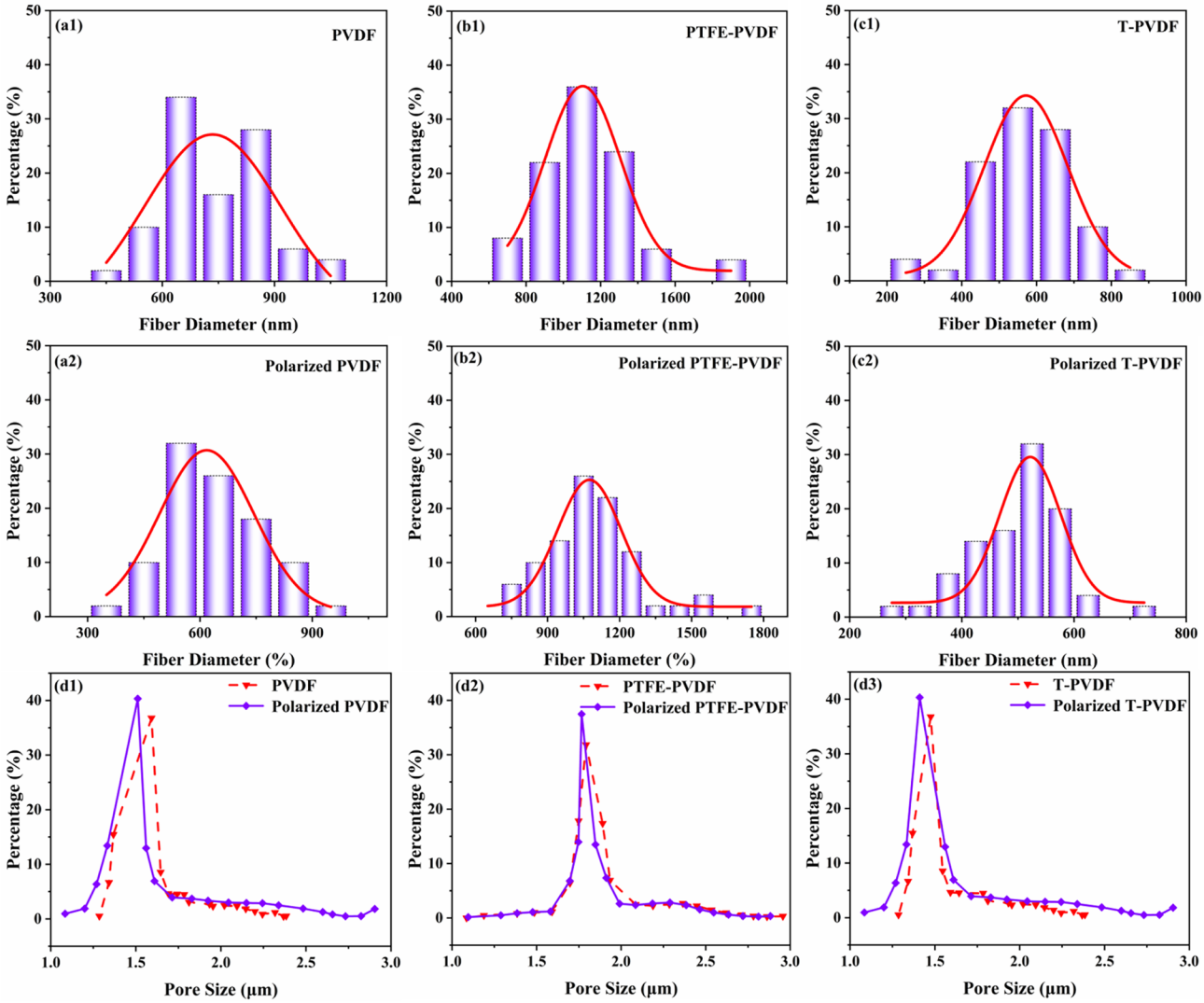

Fig. 3 The distribution of fiber diameter (**a**–**c**) and pore size (**d**) of ENMs before and after electrification treatment

Table 1 Average diameter and pore size of ENM before and after electrification treatment

Sample	Average diameter before electrification treatment (nm)	Average diameter after electrification treatment (nm)	Pore size before electrification treatment (nm)	Pore size after electrification treatment (nm)
PVDF	728 ± 133	629 ± 121	1592 ± 163	1511 ± 128
PTFE-PVDF	1125 ± 241	1086 ± 212	1793 ± 171	1766 ± 175
T-PVDF	555 ± 115	494 ± 85	1475 ± 140	1410 ± 103

− 4.0 kV, − 6.1 kV, and − 6.4 kV. Due to the accumulation of charge and oriented dipole of ENMs with the increase of charge time, the surface potential of ENMs barely raised rapidly and slowly tended to be stable.

ENMs after electrification treatment were exposed to air at 25 ℃ and relative humidity of 30%, and observed for surface potential versus exposure time, as shown as Fig. 4c. As can be seen from Fig. 4c, the surface potential of ENMs decreases rapidly in the early stage, owing to escaping of unstable substantial charges on the surface of ENMs. After a period of time, the surface potential decreases slowly and tends to be stable, because of trapped charged particles on the surface of ENMs and the covalent bonds of the macromolecules in the nanofiber. The surface potential of T-PVDF

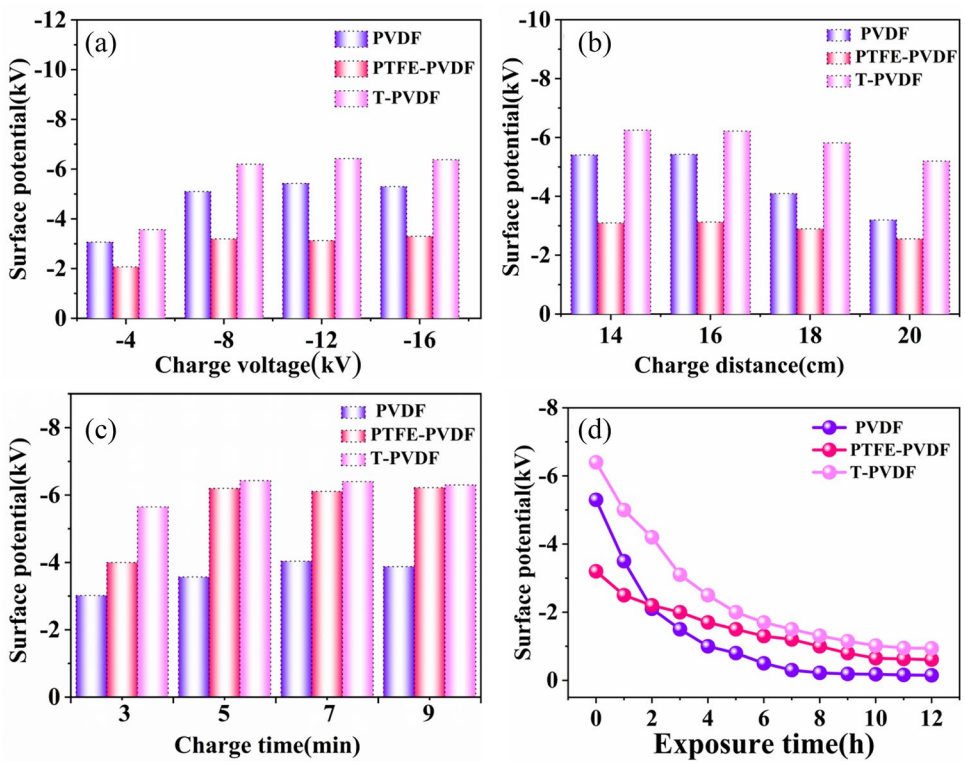

Fig. 4 Surface potential versus charging voltage (**a**), charge distance (**b**) and charging time (**c**) curves of ENM with electrification treatment. Surface potential versus exposure time curves of ENM after electrification treatment (**d**)

ENM was highest compared to those of the other samples. We speculated that a large number of electric dipoles in the tourmaline nanoparticle had not completely restored the disorder state, which were in the high orientation, resulting in the highest surface potential related to T-PVDF ENM. Even though the surface potential of T-PVDF ENM after exposure time of 12 h was just − 1 kV, it also could support strong electrostatic force to easily adsorb and quickly capture particles in the air when passing through the electret filter media, compared to ENM without electrification treatment.

The surface potential of the T-PVDF ENM is higher than that of the PVDF ENM after exposure 10 h, indicating that the high oriented electric dipoles in Tourmaline nanoparticles has not completely recovered to the disordered state. The surface potential of the PTFE-PVDF ENM is lower and decreases lowlier than that of PVDF ENM in 2 h. It is supposed to the fact that oriented electric dipoles in PTFE were harder to escape than the surface charge of ENMs. It was found that the surface potential of the three ENMs had certain durability after exposure to air for a period of time.

3.3 Filtration Performance of ENM

Figure 5 shows the filtration performance of three ENMs before and after electrification treatment. From Fig. 5a, b, it was noticeable that the filtration efficiency of unpolarized and polarized ENM increased with the increase of spinning time, and reached a stable value after a certain time. Compared with the filtration resistance broken line diagram of unpolarized and polarized ENM, it was found that the two broken lines almost coincide, indicating that the electrification treatment has no effect on the morphology of ENM. When the spinning time was 2.5 h, the filtration efficiency of the polarized PVDF ENM reached 98.97%, and the filtration resistance was 99 Pa. When the spinning time was 2.5 h, the filtration efficiency of the polarized PTFE-PVDF ENM reached 99.23%, and the filtration resistance was 88 Pa. When the spinning time was 2.5 h, the filtration efficiency of the polarized T-PVDF ENM reached 99.20%, and the filtration resistance was 89 Pa.

Since electret materials tend to lose partial charges in the air, the filtration performance of ENM after exposure to air for 12 h was tested at 25 ℃ and relative humidity 30% (Fig. 5). After exposure to the air for 12 h, the filtration efficiency of the discharged ENM was still higher than that of the uncharged ENM, which indicated that a part of the charges and oriented dipoles could be retained inside the nanofibers when subsequently used as air filter media, although accompanied with the escape of charges from fiber surfaces. It was also found that when the spinning time was 2.5 h, the filtration efficiency of the PVDF ENM after exposure to air for 12 h could reach to 98.80%, and the filtration resistance was 100 Pa. When the spinning time was 2.5 h, the filtration efficiency of the PTFE-PVDF ENM exposed to air for 12 h reached to 99.03%, and the filtration

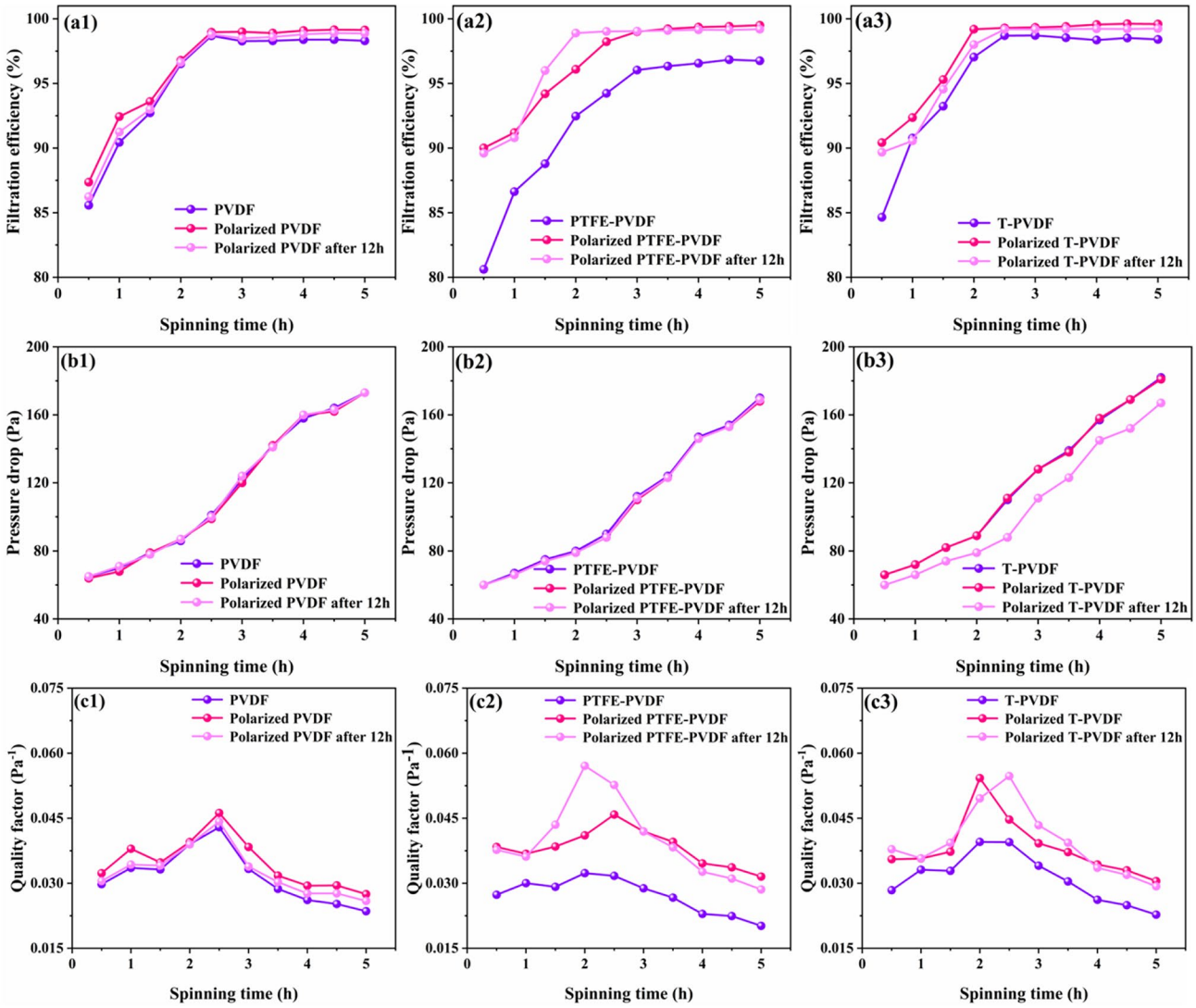

Fig. 5 The results of filtration efficiency, pressure drop and quality factor of PVDF (**a1**–**c1**), PTFE-PVDF (**a2**–**c2**) and T-PVDF (**a3**–**c3**) ENM before and after the electrification treatment

resistance was 88 Pa. When the spinning time was 2.5 h, the filtration efficiency of the T-PVDF ENM exposed to air for 12 h reached 99.19%, and the filtration resistance was 88 Pa. The results showed that the three types of ENMs after electrification treatment still have high enough semi-durable air filtration performance, even if the charges were partially lost. To comprehensively assess the filtration performance of ENMs, the QF at the air flow of 85 L/min were explored carefully. From Fig. 5c, the QF of the T-PVDF ENM with electrification treatment after exposure to air for 12 h was the highest value of 0.0547 Pa^{-1}, owing to the lower electrostatic force to trap particles, resulting the lower pressure drop.

So far, many different types of ENMs have been complexed and fabricated for improving its high air filtration properties. To evaluate the filtration performance of ENM, a comparison of FE, ΔP and QF of ENM as the air filtration media under air flow of 85 L/min in this work with those in previous studies was shown in Table 2. Compared to other ENM, electrification treatment in this work could enhance polarized T-PVDF ENM with the higher PE value, the lowest

Table 2 Comparison of FE, ΔP and QF of ENM as the air filtration media under air flow of 85 L/min in the literature and this work

Sample	FE (%)	ΔP (Pa)	QF (Pa^{-1})	References
PEI/CuMOF ENM	99.09	138	0.0341	[34]
PS/FPU/GO–GH ENM	98.86	137	0.0323	[35]
PMIA/PAN/SiO2 ENM	99.71	164	0.0356	[36]
PSA/PAN-B ENM	97.01	119	0.0295	[37]
PAN ENM	96.60	172	0.0196	[38]
Polarized T-PVDF ENM	99.19	88	0.0547	This work

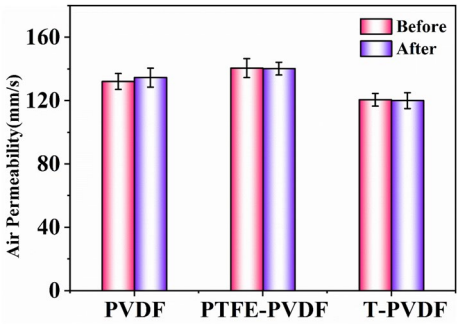

Fig. 6 Air permeability of PVDF, PTFE-PVDF and T-PVDF ENMs before and after electrification treatment

ΔP value and the highest QF value, which indicated that the effectiveness of electrification treatment for improving filtration performance was excellent. It would play a vital role in effectively defending the particulate matters in the air, when it was used as the air filtration media.

3.4 Air Permeability of ENM

Figure 6 shows the air permeability of ENMs before and after electrification treatment. In Fig. 6, the air permeability of PVDF, PTFE-PVDF and T-PVDF ENMs were 132 mm/s, 140 mm/s and 120 mm/s. Furthermore, there was no obvious change in the air permeability of ENMs before and after the electrification treatment. In fact, the pore size of ENM plays an important role in determining the air permeability of air filtration products. In Fig. 3 and Table 1, pore sizes of PVDF, PTFE-PVDF and T-PVDF ENM before electrification treatment were 1592 nm, 1793 nm and 1475 nm. While pore sizes of PVDF, PTFE-PVDF and T-PVDF ENM after electrification treatment were 1511 nm, 1766 nm and 1410 nm. As expected, pore sizes of ENMs almost unchanged after electrification treatment. A large number of charged particles were attached to the traps on the surface of the ENM and the covalent bonds of the macro-molecules in the ENM, which were generated in the process of electrospinning. At the same time, charged particles in the ENM could be highly oriented in the electric field, which had not a great impact on the pore sizes of ENM after electrification treatment, resulting in similar air permeability.

4 Conclusion

In summary, PVDF, PTFE-PVDF, and T-PVDF ENMs were prepared by combination of electrospinning and electrification treatment. The filtration performance and durability of the sample before and after electrification treatment were studied. It is found that corona charge electret has little effect on the morphologies of ENMs. After electrification treatment, the filtration efficiencies of ENMs were obviously improved, while the filtration resistance was almost unchanged. Moreover, the filtration efficiencies and filtration resistances of ENMs after exposure to the air for 12 h were still greater than 98%, and less than 100 Pa, respectively. Based on the results above, we believe that ENM with electrification treatment can be use as highly efficient, low resistant, and semi-durable air filtration media.

Acknowledgements This work was supported by National Natural Science Foundation of China (NSFC, no. 51973168) and the "Wuhan Talents Plan"- Hubei Wuhan's High Level Talents Special Support Plan (no. [2022]734).

Data availability The data that support the findings of this study are available from the corresponding author upon reasonable request.

Declarations

Conflict of Interest The authors declare that they have no known competing financial interests or personal relationships that could have appeared to influence the work reported in this paper.

References

1. H. Khreis, T. Ramani, K. de Hoogh, N. Mueller, D. Rojas-Rueda, J. Zietsman, M.J. Nieuwenhuijsen, Int. J. Transp. Sci. Technol. **8**, 116 (2019)
2. H. Khreis, K. de Hoogh, M.J. Nieuwenhuijsen, Environ. Int. **114**, 365 (2018)
3. W.J. Gauderman, H. Vora, R. McConnell, K. Berhane, F. Gilliland, D. Thomas, F. Lurmann, E. Avol, N. Kunzli, M. Jerrett, J. Peters, Lancet **369**, 571 (2007)
4. A. Maher Barbara, A. M. Ahmed Imad, V. Karloukovski, A. MacLaren Donald, G. Foulds Penelope, D. Allsop, M. A. Mann David, R. Torres-Jardón, L. Calderon-Garciduenas, *Proc. Natl. Acad. Sci.*, **113**, 10797 (2016).
5. Z.J. Andersen, L.C. Kristiansen, K.K. Andersen, T.S. Olsen, M. Hvidberg, S.S. Jensen, M. Ketzel, S. Loft, M. Sørensen, A. Tjønneland, K. Overvad, O. Raaschou-Nielsen, Stroke **43**, 320 (2012)
6. C. Zou, Y. Shi, X. Qian, J. Ind. Text. **51**, 1186S (2022)
7. J. Li, W. Wang, H. Du, X. Hu, Ceram. Int. **46**, 28742 (2020)
8. N. Deng, H. He, J. Yan, Y. Zhao, E.B. Ticha, Y. Liu, W. Kang, B. Cheng, Polymer **165**, 174 (2019)
9. H. Zhang, Q. Zhen, Y. Liu, R. Liu, Y. Zhang, Results Phys. **12**, 1421 (2019)
10. H. Xiao, Y. Song, G. Chen, J. Electrostat. **72**, 311 (2014)
11. M. Jafari, E. Shim, A. Joijode, Sep. Purif. Technol. **260**, 118185 (2021)
12. M. Sohrabi, M. Abbasi, A. Sadighzadeh, A Fabrication and evaluation of electrospun polyacrylonitrile/silver nanofiber membranes for air filtration and antibacterial activity. Polym. Bull. (2022). https://doi.org/10.1007/s00289-022-04311-1
13. Z. Chen, Y. Liu, J. Huang, M. Hao, X. Hu, X. Qian, J. Fan, H. Yang, B. Yang, Polymers **14**, 3404 (2022)
14. Z. Chen, Y. Liu, J. Huang, H. Wang, M. Hao, X. Hu, X. Qian, J. Fan, H. Yang, B. Yang, J. Funct. Biomater. **13**, 161 (2022)
15. X. Yu, C. Li, H. Tian, L. Yuan, A. Xiang, J. Li, C. Wang, A.V. Rajulu, Chem. Eng. J. **396**, 125373 (2020)

16. W. Yang, Y. Liu, X. Hu, J. Yao, Z. Chen, M. Hao, W. Tian, Z. Huang, F. Li, *Polymers*, **11** (2019).
17. H. Qiao, R. Li, Y. Yu, Z. Xia, L. Wang, Q. Wei, K. Chen, Q. Qiao, Electrochim. Acta **273**, 282 (2018)
18. Y. Liu, M. Hao, Z. Chen, L. Liu, Y. Liu, W. Yang, S. Ramakrishna, Curr. Opin. Biomed. Eng. **13**, 174 (2020)
19. J. Lannutti, D. Reneker, T. Ma, D. Tomasko, D. Farson, Mater. Sci. Eng. C **27**, 504 (2007)
20. S. Li, Z. Cui, D. Li, G. Yue, J. Liu, H. Ding, S. Gao, Y. Zhao, N. Wang, Y. Zhao, Compos. Commun. **13**, 1 (2019)
21. X. Wen, J. Xiong, S. Lei, L. Wang, X. Qin, Adv. Fiber Mater. **4**, 145 (2022)
22. Y. Su, T. Fan, W. Cui, Y. Li, S. Ramakrishna, Y. Long, Adv. Fiber Mater. **4**, 938 (2022)
23. X. Ding, Y. Li, Y. Si, X. Yin, J. Yu, B. Ding, Compos. Commun. **13**, 57 (2019)
24. Z.-X. Huang, X. Liu, X. Zhang, S.-C. Wong, G.G. Chase, J.-P. Qu, A. Baji, Polymer **131**, 143 (2017)
25. Y. Li, X. Yin, Y. Si, J. Yu, B. Ding, Chem. Eng. J. **398**, 125626 (2020)
26. Y. Li, L. Cao, X. Yin, Y. Si, J. Yu, B. Ding, J. Colloid Interf. Sci. **578**, 565 (2020)
27. N. Wang, M. Cai, X. Yang, Y. Yang, J. Colloid Interf. Sci. **530**, 695 (2018)
28. Q. Sun, W.W.-F. Leung, Sep. Purif. Technol. **240**, 116606 (2020)
29. J. V. Turnhout, W. J. Hoeneveld, J. C. Adamse, L. M. V. Rossen, *IEEE T. Ind. Appl.* **IA-17**, 240 (1981).
30. J. Van Turnhout, J.W.C. Adamse, W.J. Hoeneveld, J. Electrostat. **8**, 369 (1980)
31. C. Kanaoka, S. Hiragi, W. Tanthapanichakoon, Powder Technol. **118**, 97 (2001)
32. S. Ding, Y. Cao, F. Huang, Y. Wang, J. Li, S. Chen, Compos. Sci. Technol. **217**, 109093 (2022)
33. S. Wang, X. Zhao, X. Yin, J. Yu, B. Ding, A.C.S. Appl, Mater. Inter. **8**, 23985 (2016)
34. H. Wu, Z. Hu, Q. Geng, Z. Chen, Y. Song, J. Chu, X. Ning, S. Dong, D. Yuan, Colloid. Surf. A **651**, 129656 (2022)
35. W. Shao, Y. Zhang, N. Sun, J. Li, F. Liu, J. He, A.C.S. Appl, Nano Mater. **5**, 13573 (2022)
36. Q. Geng, Y. Pu, Y. Li, X. Yang, H. Wu, S. Dong, D. Yuan, X. Ning, J. Hazard. Mater. **422**, 126835 (2022)
37. X. Yang, Y. Pu, S. Li, X. Liu, Z. Wang, D. Yuan, X. Ning, A.C.S. Appl, Mater. Inter. **11**, 43188 (2019)
38. R. Al-Attabi, L.F. Dumée, L. Kong, J.A. Schütz, Y. Morsi, Adv. Eng. Mater. **20**, 1700572 (2018)